

UNIVERSITY OF TORONTO

PHYSICS 479: FINAL REPORT

APPLICATIONS OF CONTROL THEORY TO AN ULTRACOLD ATOMS  
EXPERIMENT

---

# Digital Feedback Systems for Optical Traps

---

*Author:*

Andrew HARDY

*Professor:*

Dr. Aephraim STEINBERG



## Abstract

This report will detail the creation and testing of a digital feedback circuit for laser power in the context of the Bose Einstein Condensate. I will begin with an analysis of the current analog feedback systems in place for the system. From this position, I will motivate the need for upgraded digital feedback loops. In particular, I will focus on the delta-kick cooling [12] [5] laser and its unique requirements suited to a digital feedback system. The bulk of the report will then illustrate the progress made towards realizing a digital feedback system for delta kick cooling or other applications.

## 1 Introduction

Bose-Einstein Condensation (BEC) was theorized in 1925 by Albert Einstein [8] after correspondence with Satyendra Nath Bose [7]. BEC is a state of matter where almost all the particles in a boson gas occupy the lowest energy level. This dense occupation means the atoms have a cooperative effect, behaving more like an individual particle than a collection of particles. The significance of this is that the condensate has a De-Broglie thermal wavelength  $\lambda = \frac{h}{p}$  long enough to have macroscopic effects. This makes their quantum wave character apparent. In 1995, a team of scientists at JILA led by Eric Cornell and Carl Wieman realized a BEC. [6] This discovery allowed BEC to become a powerful tool in probing quantum questions.

The BEC group in Dr. Aephraim Steinberg's laboratory at the University of Toronto aims to measure one of the most fundamental and peculiar quantum effects, quantum tunneling. [11] Quantum tunneling is the existence of a particle wave function existing on both sides of a potential barrier, in classically 'forbidden' regions. Because of the large BEC wavelength, it becomes an ideal tool to study quantum tunneling dynamics. One of the most fundamental components of these dynamics, the time it takes for a particle to tunnel, remains an open question. I will provide a broad overview of one of the optical set-ups required to explore that question. Through this, I will motivate the need to a digital feedback circuit.

## 2 Current Set-Up and Motivation

This work begins with Rubidium-87 atoms released from a BEC trap traveling towards an optical barrier through an optical waveguide. This BEC is in the nanokelvin temperature regime, with the vast majority of the atoms at their ground state. However, in order to perform tunneling experiments, we also require these atoms to be cold in the more traditional sense, in terms of kinetic energy. This means that we need to develop a technique to reduce their momentum distribution.

### 2.1 Optical Dipole Traps

The current waveguide for Rb atoms operates at 1064nm and serves as an Optical Dipole Trap (ODT). The classical macroscopic equivalent are optical tweezers, for which the 2019 Nobel Prize for Physics was awarded.

ODT operate on the electric dipole interaction with far-detuned light, much weaker than other neutral atom trapping. However, as mentioned later, they do not suffer from effects of radiation pressure. [9] Far-detuned light ( ‘red’ detuning,  $\delta < 0$  ) causes a negative dipole potential, attracting atoms. This dipole potential means the Hamiltonian of the system must be considered in terms of both the atom and the electric field of the laser. By applying second-order perturbation theory to this ‘dressed’ state, the potential optically induces a shift in the energy levels. This phenomenon is referred to as an AC Stark Shift.

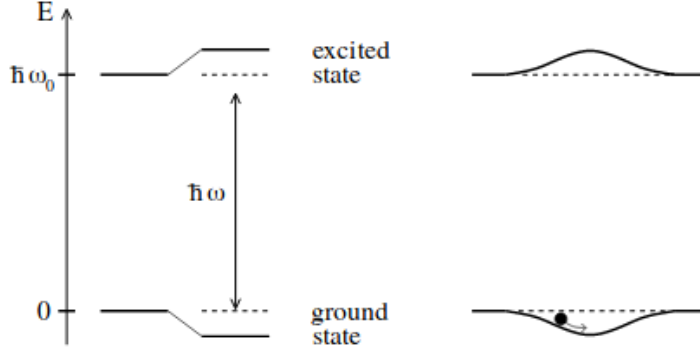


Figure 1: A diagram [9] of optical energy shifts (AC Stark Shift) for a two-level atom. Red-detuned light lowers the ground state and raises the excited state up by same amounts. A spatially inhomogenous electric field, like a Gaussian laser beam, creates a ground-state potential well, trapping the neutral atom

I now consider a strongly focused Gaussian laser beam. As laser light from a fibre can be approximated as Gaussian, this is an accurate derivation for the waveguide ODT. The intensity of this beam varies across the transverse from the focus following the expression  $I(r) = I_0 e^{-r^2/w_0^2}$ . [10].  $w_0$ , the minimum beam radius, is referred to as the beam waist.  $I_0$ , the initial intensity at the focus, is defined in terms of the power and beam waist as  $I_0 = \frac{2P}{\pi w_0^2}$ . This red-detuned laser, gives an everywhere negative ground-state light shift, maximizing at the centre of the Gaussian beam. Ground state atoms experience an attractive force towards the centre. This force is given by the gradient of the light shift. The AC Stark shift, given in terms of the Rabi frequency and detuning is  $\Delta E_g = \frac{\hbar \Omega^2}{4\delta}$ . In the limits where  $|\delta| \gg \Omega$  and  $|\delta| \gg \gamma$ , (where  $\gamma$  is the natural atomic line-width), the force is expressed as

$$F \simeq -\frac{\hbar}{4\delta} \nabla (\Omega(r)^2) = -\frac{\hbar \gamma^2}{8\delta I_s} \nabla I(r) \quad (1)$$

where, the Rabi Frequency is given in terms of natural width, intensity and saturation intensity as  $\Omega^2 = \gamma^2 I/2I_s$ . Therefore, by computing the gradient, we receive the expression [10].

$$\mathbf{F} \simeq \frac{\hbar \gamma^2}{4\delta} \frac{I_0}{I_s} \frac{r}{w_0^2} e^{-r^2/w_0^2} \quad (2)$$

In addition, tuning of the laser parameters allow for longitudinal and therefore 3D atomic trapping. This tuning consists of a sufficiently large detuning which decreases the radiation pressure faster than the dipole force. The radiation pressure of the laser beam scales  $\frac{1}{\delta^2}$  compared to the dipole force scaling with  $\frac{1}{\delta}$ . Atoms therefore spend only a small time in the excited / repelled state and are effectively trapped.

### 2.1.1 Current Analog Feedback

AS the force on the atoms is directly proportional to the power of the laser beam, we require precise power control. The current power feedback set-up succeeds at this for the optical waveguide. The system takes diverted laser optical power from an Acousto-optic modulator (AOM). This is fed into a photodiode. This current is passed through a resistor and the voltage across this resistor is read by a analog PI box. This box has a notable disadvantage that the gain of the Proportional and Integral components, in series, are coupled, limiting the tun-ability of the circuit. The time parameter of the integral component is also determined by a hardwired capacitor. This prevents any tun-ability. The PI box outputs a voltage between 0 and 1 V into an AOM driver. The optical power has a nonlinear response to the AOM RF power, but through empirical testing based on the response to the atomic cloud, the system works. However, for systems that require higher bandwidth than the waveguide, this analog device fails to provide adequate control. This makes the next section a prime candidate for a new digital feedback circuit.

## 2.2 Delta Kick Cooling

Delta-Kick Cooling (DKC), otherwise known as matter-wave lensing, serves to lower the effective temperature of atoms by collimating the atomic cloud. By separating atoms by their velocities, the velocity distribution width, and therefore the temperature, is incredibly low. This process serves as the temporal matter-wave analog to an optical lens [12]. [5] The process can be described using a Hamiltonian  $H_0 = p^2/2m + U(x)$ . By extinguishing the

potential and subsequently pulsing it, provides a new Hamiltonian,

$$H_k = \frac{p^2}{2m} + V(x)\delta(t - T) \quad (3)$$

The new potential, defined with a Gaussian time pulse,  $\exp [-(t - T)^2/2\tau_p^2]$ , defines the new potential as  $\sqrt{2\pi}\tau_p U(x)$  where  $\tau_p$  is the temporal pulse width. As we extinguish  $U(x)$ , the atoms gain a spatial spread based on momentum differences. Given sufficient time( $T$ ), the momentum of atoms will effectively be a linear function of position,  $p = mx/T$ . By establishing the pulse width based on the free expansion time of the atoms absent of potential, each kick reduces the momentum of every atom near zero. This occurs given the following condition, described in terms of the frequency of the harmonic potential,

$$\kappa_{cl} = \sqrt{2\pi}\tau_p\omega^2 T \approx 1 \quad (4)$$

This classical description does not give a complete picture of the process, but is sufficient to serve as motivation. As a brief aside, in the quantum mechanical picture, DKC serves to broaden the position wave function  $\psi(x)$ , but narrow the width of the momentum  $\phi(p)$  by a factor  $Q$  and lower the energy, and effective temperature, by  $Q^2$ . From this rough treatment, the need for precise power control on the DKC beam becomes apparent. Our DKC procedure consists of two kicks, the first for 1ms, and the second, 15ms later, with half the power. In these narrow time scales, high bandwidth (on the order of 100KHz) of a feedback system would be critical for accurate power control.

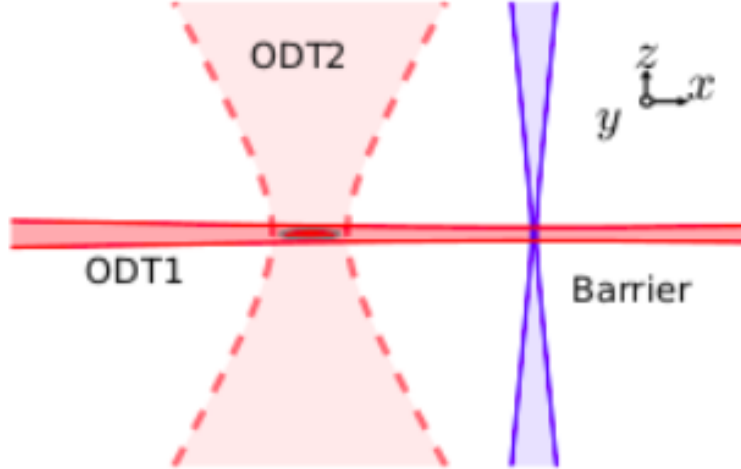


Figure 2: A diagram [12] detailing the three beams described in this section. ODT1 serves as the wave-guide. ODT2 serves as the DKC beam, and the optical barrier beam is also shown.

### 3 Present Progress

The current digital feedback circuit (DFC) consists of three components. It begins with an analog to digital conversion (ADC) pin on the chipKIT uC32 micro-controller. This device reads a digital representation of the voltage taken across a resistor connected to the photo-diode. The device then computes a digital correction value using digital PID software. This correction value is converted into binary and fed across the Serial Port Interface (SPI) channels into the digital to analog convertor, an Analog Devices 5780 Evaluation Board. Based on the configuration of that SPI and the DAC itself, it will output a voltage. The following sections will describe in detail the mechanisms of these three components.

#### 3.1 Analog to Digital Conversion

For all experimental concerns, the ADC on the uC32 serves as a black box. However it also serves as the main limiting factor on the bandwidth of the whole DFC, so it warrants adequate explanation. On the uC32, Pins numbered 14 – 25 or A0-A11 serve as possible

analog inputs. They are in the J7, or ANALOG section of the board. Together with the GND pin, located in J2 or POWER section of the board, analog input is quite simple. [3] The Arduino Library allows analog input via calling of two functions to specify the pin setting and read out an integer value.

```
pinMode(A0, INPUT);
analogVal = analogRead(A0);
```

This integer value reads with 10 bit precision the voltage value between 0 – 3.3 V. The conversion therefore follows the formula

$$V_a = \frac{3.3V_d}{1023} \quad (5)$$

which gives the analog voltage reading in terms of the integer output.

The mechanics of the ADC operate on the principles of successive approximation. [4] This operates through a comparator comparing voltage inputs to voltages coming from a small DAC present in the chip in order to receive an accurate value of the true voltage. On the uC32, the PIC32 processor operates ADC as follows. The analog input is fed through two multi-plexers (MUXs) to one Sample and Hold circuit (SHA). This allows the MUXs to switch between different analog input pins. The SHA then sends the voltage through a Successive Approximation Register (SAR) through which the actual conversion occurs.

### 3.1.1 ADC Speed

The conversion is supposed to take 12 clock cycles. One clock cycle for each bit of resolution of the voltage and two clock cycles to complete the conversion. The uC32 operates at 80Mhz, so we should expect approximately 6.6 Mhz conversion rate. The datasheet boats 1Mbps though. If this means that the pins only sample at 1Mhz, then the conversion rate is only 83 Khz. Experimental testing confirms that the rate is within this order of magnitude.



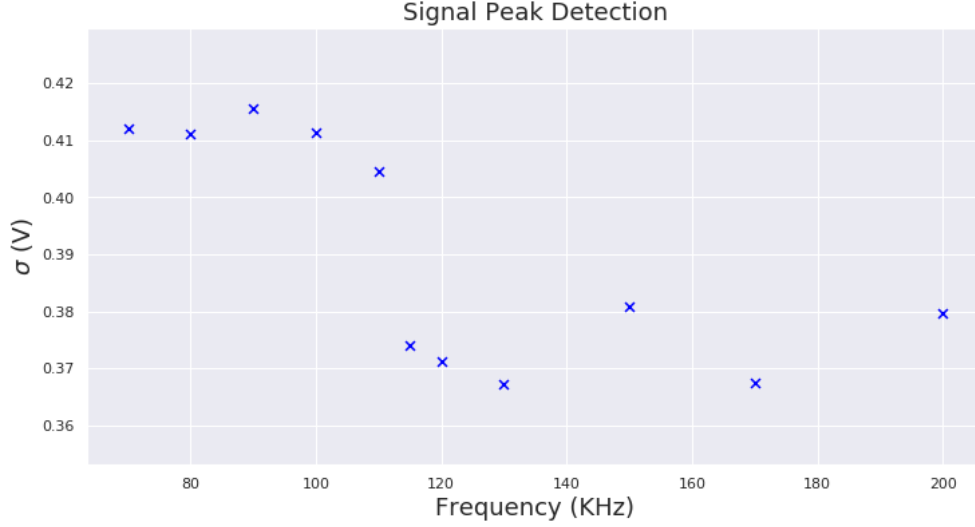


Figure 3: Peak Identification of Sine Wave: Here the standard deviation  $\sigma$  of a sin wave is compared to the frequency of the sin wave.  $\sigma$  serves as roughly the peak of a sine wave. While the signal was set to 0.4V on the Function Generator, due to sampling times, this was incorrectly read above the 100KHz regime.

### 3.2 PID Controller

The beginning of any study of control theory begins with PID. For the past century, it remains one of the most robust methods to stabilization and control. The basics of PID are the three parameters used in error correction. Given the formula

$$u(t) = K_p e(t) + K_i \int_0^t e(t') dt' + K_d \frac{de(t)}{dt} \quad (6)$$

they are  $K_i, K_p, K_d$ , standing for the Proportional, Integral and Derivative. All three of these components serve critical roles in accurate control. I will give brief explanations of the uses of all three of the parameters in the context of laser power control. Then I will give an overview of how to tune the parameters and some progress made in PID simulations in order to best understand the PID.

### 3.2.1 Parameters and the Ziegler-Nichols Method

The first, and most significant parameter is the proportional gain. This is a simple weight on the error given,  $e(t) = S - I(t)$ , the difference between the setpoint value and the input signal with noise. If a device had infinite bandwidth, this instantaneous (or instantaneous compared to the speed of noise and drift) correction would wash out the noise and a P controller would be sufficient. Instead, most P control only allows the signal to oscillate around the set point. Every correction misses the mark because of the delay between the read signal and the correction output. In order to remedy this oscillation, the Integral gain allows for a discrete integral accumulation of error measurements. This allows the PID to make cumulative measurements and correct drift in the error signal. This parameter therefore serves to damp the oscillations.

PI controllers serve a large majority of the control community adequately. However, when the error source becomes much more variable, adequate control requires an additional parameter. This is the Derivative gain. Rather intuitively, this gain gives some predictive ability of the error. Derivative gain allows the PID to correct for error that will appear in the signal by the time that the PID outputs a correction. Because of these time sensitivity concerns, it is worth noting that the sampling rate of the integral and derivative components serve to be just as essential. In order to tune these parameters, one of the most robust heuristic methods is dubbed Ziegler -Nichols [13]. It consists of fixing the  $K_p$  gain until there are steady oscillations, and then tweaking  $K_i$  and  $K_d$  in order to damp these oscillations. The Ziegler-Nichols method prescribes specific values based on the response of the system.

The difficulty with our laser power control set-up deals with the response time of the AOM and bandwidth of the total system. Because the AOM driver only takes 0 to 1 volts, it will require more nuanced PID tunings because there is no subtraction of power. In addition, the AOM will have improved functionality if the input voltage does not oscillate too rapidly.

### 3.2.2 Results of PID Simulation

In order to understanding the workings of a PID, I explored the Arduino PID library using simulations. The equation used in the simulation was

$$x_i - x_{i+1} + \frac{1}{5} \sin(10t) + g\omega + n \quad (7)$$

which includes a sinusoidal noise term, a random noise ,  $n = \pm 1$ , and the output  $w$  multiplied by some gain factor  $g = 1/40$ . These values are coded in terms of pure values, not yet converted into voltages.

The behavior of the system follows the expected results of Ziegler Nichols. Once an appropriate gain for the total output was established, relatively naive  $K_i, K_d$  parameters were able to control the system. Then through tweaking, a more gentle control system was established.

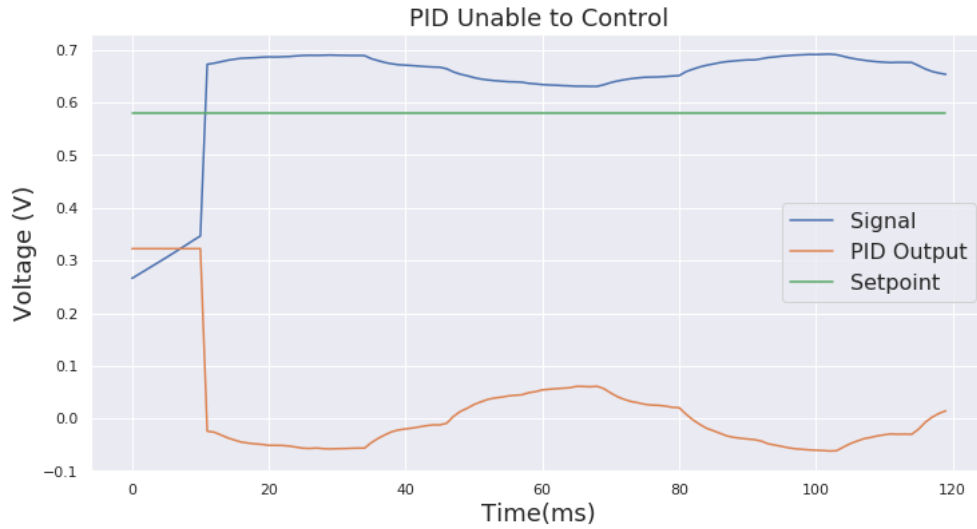


Figure 4: Feedback System with Naive Parameters. The parameters were set to  $K_p = 2, K_i = 0, K_d = 0$ . This was unable to reach the setpoint.

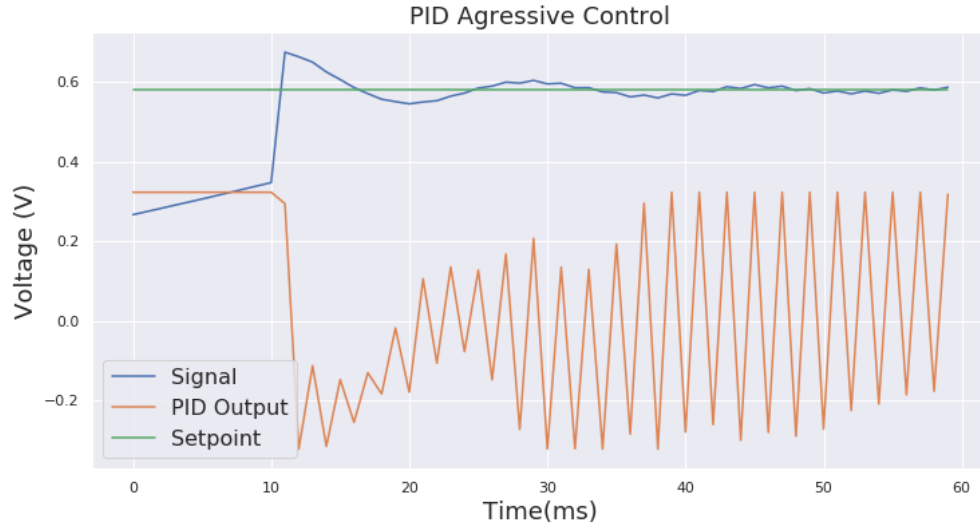


Figure 5: Feedback System with Naive Parameters. The parameters were set to  $K_p = 2$ ,  $K_i = 4.5$ ,  $K_d = 4$ . Notice the extreme oscillations of the PID output.

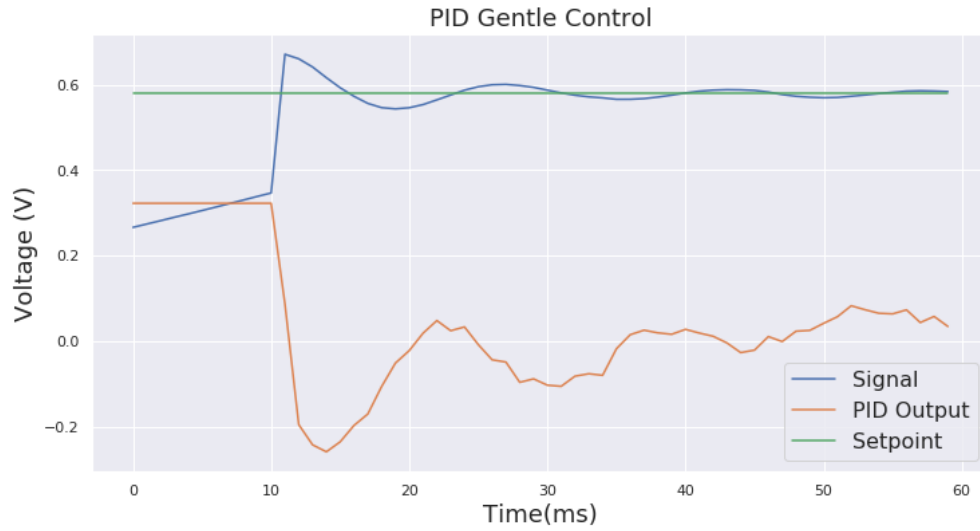


Figure 6: Feedback System with Tuned Parameters. The parameters were set to  $K_p = 2$ ,  $K_i = 4.5$ ,  $K_d = 2.7$ . Notice similar signal behavior but less aggressive control.

### 3.3 Digital to Analog Conversion

The least interesting, but most difficult component of the entire feedback circuit rests in the actual conversion from a digital number to an analog voltage used to drive the AOM. Our current Digital to Analog Converter (DAC) is an Analog Devices AD5780 mounted to an evaluation board. The evaluation board contain several particular Links, denoted by LK. These links determine several important settings for the AD5780. The ones changed from the default are documented here.

Table 1: LK Settings on AD5780

LK	VSetting
LK1 Position B	Digital Power Supply now J1
LK2 Position A	On board Positive reference +5V
LK7 attached	LDAC at logic Low
LK8 Position B	On board negative reference AGND
LK11 Removed	DAC accesible at VOUT instead of VOUT Buffered

The current configuration requires two voltage sources. 5V and a ground are supplied to J1, denoted by VCC and DGND. These power the AD5780 IC itself. In addition, voltages anywhere in the range of  $\pm(7.5 - 16)V$  must be supplied to J2. Positive voltage is between VDD and AGND while negative voltage is between VCC and AGND. These voltages serve as the reference voltages read by the AD5780.

The next configuration requirement is the actual SPI pins. The SPI communication requires 6 different pin connections. The crux of SPI communication is that a tremendous amount of logical information is able to be sent over a single pin through syncing the logical bits to clock cycles. SPI functions through a Master-Slave relationship. The Master Device, here the micro-controller, sets a Slave Select (SS) pin low to determine the other device is a Slave. The AD5780 also requires the LDAC pin to be set low while data is transferred. While these pins are held low, Information is either sent through the Master Out, Slave In (MOSI) pin,

or through the Master In, Slave Out, (MISO) pin. These are synced to a CLCK pin. The sixth pin is DGND.

Table 2: SPI Pins

uC32 Pin Number	SPI Connection	Colour
10	SS	Green
11	MOSI	Red
12	MISO	Orange
13	CLCK	White
9	LDAC	Blue
6	DGND	Black

SPI has four modes for how the SPI is configured to the clock cycle. the CPOL bit represents the clock polarity. If this is 0 or 1 means the clock is idle when high or low. Meanwhile the CPHA bit represents clock phase. This represents if the data is shift out on the rising or falling edge. [2] [?] For the AD5780, it requires data sampled on the falling edge and shifted out on the rising edge. This corresponds to CPHA = 1 and CPOL either 0 or 1. These are referred to by AD as SPIMODE 1 or 2 and by Arduino as SPIMODE 1 or 3. In order to establish these parameters, the AD Drivers call a C++ program titled Communication.cpp. The mode is established as following in a module titled SPIInit

```
{
    int spiMode = 1;
    if(clockPol == 0) {
        spiMode = clockEdg ? SPI_MODE1 : SPI_MODE0;
    } else {
        spiMode = clockEdg ? SPI_MODE3 : SPI_MODE2;
    }
}
```

SPIInit calls the Arduino SPISettings module, which determines all the important settings for SPI communication. The current settings has been changed to CPHA = 0 , CPOL = 1, for SPI\_MODE1, which is the requested information transfer for the AD5780. In addition, the DAC has a maximum clock speed of 35MHz, so the clock speed is set to 20MHz, a quarter of the processor clock on the uC32, but well above the limiting bandwidth of the ADC. The DAC also takes the most significant bit (MSB) first.

The data itself is sent to four different registers. This is established via the first four bits sent into the AD5780. The first bit R/W is set to 1 for writing to the AD5780. The next three bits establish the address for the register information is being sent to.

An advantage of the AD drivers currently in implementation is that these addresses are established in the header files called, rather than needing to be defined by the user. The current software calls the CTRL register to initialize the AD5780 and then the CLEAR register to establish a zero value voltage for the DAC. Within the loop, the voltage values are then sent to the DAC register to output voltages. The actual output voltage follows the formula [1]

$$V_{OUT} = \frac{(V_{REFP} - V_{REFN}) \times D}{2^{18}} + V_{REFN} \quad (8)$$

where the reference voltages are determined by inputs to J2 and LK2 and LK8 defined above. There is a fourth register, not used, which allows some program-ability in lieu of setting LDAC or SYNC pins. All of these registers take 18 bits of information and discard the last 2. The current drivers store these 24 bits of information in a 4 byte integer. A current unresolved bug lies in the extra byte of empty values seems to be interfering with the order of the data being transferred. the conclusion from PERC is that the chipKIT compiles the the transferred data bytes differently than the Arduino does.

## 4 Future Work

Once the DAC is up and running, the exciting parts of the digital feedback system would begin.

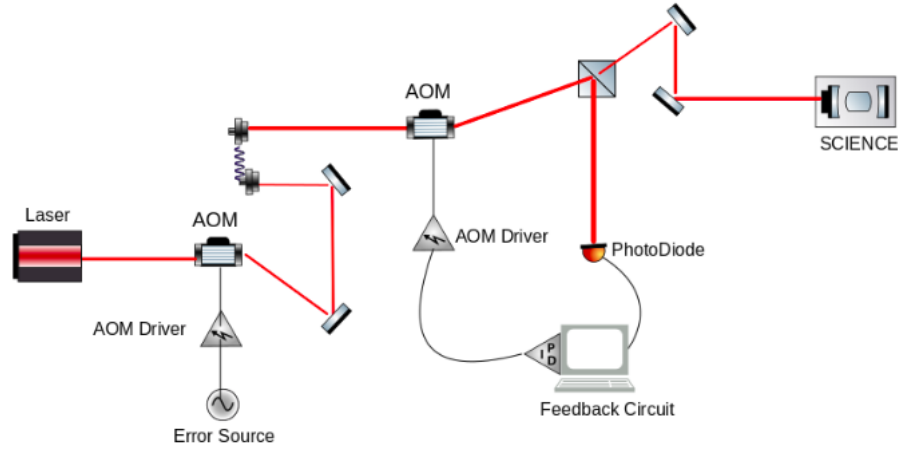


Figure 7: A diagram illustrating the ideal test set up. An additional AOM provides simulated noise which can be corrected via the digital feedback circuit set-up shown on the right hand side.

In order to realize this experimental set-up, the current lab requires development of an working laser diode with temperature and power stabilization. Then would be considerable optical table set-up. The diagram notes two mirrors at positions where fibre coupling is necessary because both position and angle need to be corrected.

Once the experimental set-up is established the PID needs to be tuned. While the Ziegler–Nichols heuristic method mentioned in Section 3.2.1 would be sufficient, the Arduino library has additional potential through the AutoTune Library. While this has no documentation or commented code, it has an active Google Groups forum. Auto-tuned PIDs take information about the peak height and frequency of the correction signal in order to extrapolate the required aggressiveness of the PID control. The library, if realized, also allows for more accurate detection of extrema in the noisy signal, and allows for tunable noise thresholds. All of these combined allow for a more accurate and more stable output signal. This has tremendous advantage if there turn out to be delays in AOM responsivity time.



## 5 Conclusion

In conclusion, digital feedback systems remain a powerful tool to improve the performance of laser cooling systems present in the current BEC experiment. Realizing these systems would lead to more accurate data and perhaps more significant scientific results. A particular advantage of digital feedback systems would be the increased bandwidth. These smaller time scales would allow for feedback on laser beams present only for 1ms. Because of this, a particular application of this digital feedback circuit would be for DKC.

## References

- [1] Ad5780 reference manual.
- [2] Arduino spi reference manual.
- [3] chipkit uc32 reference manual.
- [4] Pic32 reference manual.
- [5] Hubert Ammann and Nelson Christensen. Delta kick cooling: A new method for cooling atoms. *Physical Review Letters*, 78(11):2088–2091, 1997.
- [6] M H Anderson, Ensher, Matthews, Weiman, and E A Cornell. Observation of bose-einstein condensation in a dilute atomic vapor. *Science*, 269(5221):198–201, Jul 1995.
- [7] Bose. Plancks gesetz und lichtquantenhypothese. *Zeitschrift for Physik*, 26(1):178–181, 1924.
- [8] Albert Einstein. Quantum theory of a monoatomic ideal gas. *Physikalisch-mathematische Klasse*, 1925.
- [9] Rudolf Grimm, Matthias Weidemuller, and Yurii Ovchinnikov. Optical dipole traps for neutral atoms. *Advances In Atomic, Molecular, and Optical Physics*, page 95–170, 2000.

- [10] Harold J. Metcalf and Peter Van der Straten. *Laser cooling and trapping*. Springer, 2002.
- [11] Shreyas Potnis. *Tunneling Dynamics of a Bose-Einstein Condensate*. PhD thesis, 2016.
- [12] Ramón Ramos, David Spierings, Shreyas Potnis, and Aephraim M. Steinberg. Atom-optics knife edge: Measuring narrow momentum distributions. *Physical Review A*, 98(2), 2018.
- [13] Tim Westcott. Pid without a phd. *Embedded Systems Programming*, page 86–108, Oct 2000.